

Electron transport in a one-side-modulation-doped single-quantum-well structure: Remote-ion-scattering contribution

N. M. Cho, S. B. Ogale,* and A. Madhukar

Department of Materials Science and Physics, University of Southern California, Los Angeles, California 90089-0241

(Received 13 April 1987)

Low-temperature electron mobility limited by remote ionized impurity scattering in a one-side-modulation-doped single-quantum-well structure is calculated employing the memory-function approach. The calculations include self-consistent band-bending effects and the evaluation of quantum states and wave functions. The dynamic response of the quasi-two-dimensionally confined carriers is incorporated via use of an appropriate screening function. The dependence of the mobility on the thickness of the spacer layer, the width of the quantum well, the dopant density, and the electron concentration in the well is examined and interesting features concerning quantum-size effects are brought out for situations of current experimental interest.

I. INTRODUCTION

In recent years there has been considerable emphasis on the development of new man-made semiconductor structures which could generate novel electronic and optical responses of significance to microstructure and nanostructure devices.¹⁻⁴ Amongst the important physical properties of such structures, carrier transport has attracted special attention⁵⁻¹⁷ since it determines the speed of electronic devices which is a critical factor in evaluating their performance. Significant progress has been made in achieving high carrier mobility in man-made semiconductor structures through the introduction of the idea of modulation doping which physically separates the carriers from their parent ionized dopants,⁵⁻⁷ thus leading to an enhancement of average scattering time by orders of magnitude. In GaAs/Al_xGa_{1-x}As(100) heterostructures with the latter material grown on the former, (the so-called normal interface) and modulation doped with a spacer layer of ~ 200 Å, mobilities as high as 2×10^6 cm²/V sec have already been achieved.^{2,8} These are close to the highest values predicted by calculations.¹⁸ In spite of a number of attempts however, such high mobilities have not yet been attained in inverted (GaAs grown on Al_xGa_{1-x}As) heterostructures¹⁴⁻¹⁷ and in single-quantum-well structures,¹⁹⁻²¹ which always involve one inverted interface. The observation of relatively low mobilities in these structures is attributed to the structurally and chemically rough nature of the inverted interface and the possibility of dopant diffusion (and/or segregation) towards the inverted interface.^{17,19-22} It is now recognized that both these effects are tied to the kinetics of growth of GaAs on Al_xGa_{1-x}As and of dopant motion. Since single-quantum-well structures offer the possibility to better tailor quantum states via band-offset engineering as compared to the heterostructure case, it is of interest to examine whether high electron mobility can be achieved in such a structure by getting over the inverted interface problem. One suggestion in this context is to dope only on the side of the normal interface so as to

bypass the problem of impurity segregation at the inverted interface.^{23,24} Also, since the dopant- and carrier-generated fields in such a structure will pull the majority-carrier wave function away from the structurally and chemically rough inverted interface and towards the higher-quality normal interface, the influence of such other interface-roughness-related scattering mechanisms on the carrier mobility can also be expected to weaken. It should be pointed out, however, that since in this case the wave function is pulled towards the ionized dopants on the side of the normal interface, the corresponding contribution may undergo some increase as compared with the case of both-side doping for which the ground-subband wave function is centered at the origin. These complications thus call for a systematic study of the influence of individual scattering mechanisms on the carrier mobility in a one-side-doped single-quantum-well structure, which happens to represent a situation intermediate between a heterostructure and a double-side-doped quantum well. In the work reported in this paper we examine the influence of remote ionized donor impurities on the low-temperature electron mobility in one-side-doped Al_{0.33}Ga_{0.67}As/GaAs/Al_{0.33}Ga_{0.67}As single-quantum-well structures. We calculate the ionized-donor and carrier-generated potentials along with the carrier wave functions in a fully self-consistent calculation using exchange and correlation potentials.^{25,26} We use the memory-function approach,²⁷⁻³⁰ which intrinsically incorporates what may be called the self-energy and vertex corrections in a diagrammatic analysis of the response function, to obtain an expression for conductivity valid for arbitrary frequencies of applied field and the value of sample temperature. Having thus improved over the Boltzmann-transport-equation approach,²⁷ we study the systematics of low-frequency and low-temperature mobility by explicitly calculating the dependence of the mobility on spacer width, well width, carrier density, etc. We use a screening function appropriate for quasi-two-dimensionally confined carriers³¹ [and not a function for pure two-dimensional (2D) confinement as used in some calculations on heterostruc-

tures and double-side-doped wells] to obtain the effective scattering potential experienced by the carriers. We restrict the parameter space to cases for which no higher subband effects are of any major significance. In the following, we first discuss the method of self-consistent calculation of wave functions and confinement potential, then the mobility calculation within memory-function approach, and finally the results.

II. THEORY

A. Self-consistent calculation for potentials and wave functions

The self-consistent solutions for potential distributions and wave functions can be obtained by solving the coupled Schrödinger and Poisson equations given by^{26,32-35}

$$\frac{-\hbar^2}{2m^*} \frac{d^2}{dz^2} \eta_i(z) + V(z)\eta_i(z) = E_i(z)\eta_i(z) \quad (1)$$

and

$$\frac{d^2\phi(z)}{dz^2} = \frac{4\pi e}{\kappa} \left[\sum_i N_i |\eta_i(z)|^2 - \rho(z) \right] \quad (2)$$

with

$$V(z) = -e\phi(z) + V_{XC}(z) + \Delta E_c \Theta(z) + \Delta E_c \Theta(-z - d_w). \quad (3)$$

Here, z represents the position coordinate in the quantum-well growth direction; $V(z)$ is the z distribution of the potential comprising of the electrostatic term $-e\phi(z)$, the exchange correlation term $V_{XC}(z)$, and the band offset terms [ΔE_c is the conduction-band discontinuity and $\Theta(z)$ is the unit step function]; $\eta_i(z)$ is the normalized electron wave function for the i th subband, E_i is the energy of the i th subband; N_i is the areal electron concentration in the i th subband (cm^{-2}); $\rho(z)$ is the

z distribution of ionized dopants; m^* is the electron effective mass (in the calculations taken to be $0.065m_e$, the value for GaAs); and κ is the dielectric constant of the quantum-well structure (in the calculations assumed to have a value of 13.0, which corresponds to GaAs).

We choose the following form for the exchange and correlation potential:²⁶

$$V_{XC}(z) = -[1 + 0.7734x \ln(1 + x^{-1})](2/\pi\alpha/\gamma_s)R^* \quad (4)$$

in which, $\alpha = (4/9\pi)^{1/3}$, $x = x(z) = \gamma_s/21$,

$$\gamma_s = \gamma_s(z) = \left[\frac{4}{3}\pi(a^*)^3 n(z) \right]^{-1/3} \quad (5)$$

with

$$a^* = \frac{\kappa\hbar^2}{m^*e^2}, \quad R^* = \frac{e^2}{2\kappa a^*} \quad (6)$$

and

$$n(z) = \sum_i N_i |\eta_i(z)|^2. \quad (7)$$

Here, N_i is given by^{26,33}

$$N_i = \frac{m^*k_B T}{\pi\hbar^2} \ln \left[1 + \exp \left(\frac{E_F - E_i}{k_B T} \right) \right] \quad (8)$$

with E_F as the Fermi energy and k_B the Boltzmann constant. We work within the so-called depletion approximation which assumes that all donors are ionized in the depletion region ($z_1 \leq z \leq z_2$, see Fig. 1) and that the depleted charge density N_{dep} for $z < z_1$ is $5 \times 10^{10} \text{ cm}^{-2}$, which corresponds to an impurity concentration $N_A - N_D$ of $\sim 10^{14} \text{ cm}^{-3}$; N_A and N_D being the acceptor and donor concentrations.

The procedure of numerical calculation begins by calculating the conduction-band potential at $z \geq z_2$ for a finite temperature ($T = 4.2 \text{ K}$), using the equation given by^{34,35}

$$\phi(z \geq z_2) = k_B T \ln \left[\frac{-(1 - N_D/4N_C) + [(1 - N_D/4N_C)^2 + 4gN_D/N_C]^{1/2}}{2g} \right], \quad (9)$$

where

$$g = 2 \exp(eE_d/k_B T). \quad (10)$$

In our calculations we used a value of 50 meV for E_d which represents the donor binding energy. In Eq. (9) N_C is the equivalent density of states of the conduction band in $\text{Al}_{0.33}\text{Ga}_{0.67}\text{As}$. The boundary conditions used to solve the Poisson equation in the depletion region within the attendant framework of assumptions are

$$V(z = z_2) = -e\phi(z = z_2), \quad dV/dz|_{z=z_2} = 0. \quad (11)$$

The thickness of the space-charge region (d_{dep} , see Fig. 1) is determined by the charge-neutrality condition,

$$N_d d_{\text{dep}} = N_s + N_{\text{dep}} \quad (12)$$

with N_s being the electron concentration (per cm^2) and the equation

$$-e\phi(z = z_1) = -e\phi(z = z_2) + \frac{2\pi e^2}{\kappa} N_D (d_{\text{dep}})^2. \quad (13)$$

Correspondingly, the magnitude of the electric field at $z = z_1$ is given by

$$F(z = z_1) = \frac{4\pi e (N_{\text{dep}} + N_s)}{\kappa}, \quad (14)$$

where the penetration of the wave function in the region $z > z_1$ is ignored. At equilibrium, the Fermi level must be aligned throughout the whole region. Thus at a fixed doping concentration, N_s and d_{dep} are determined by the charge neutrality and the equilibrium condition by solving Eqs. (1)–(14) self-consistently.

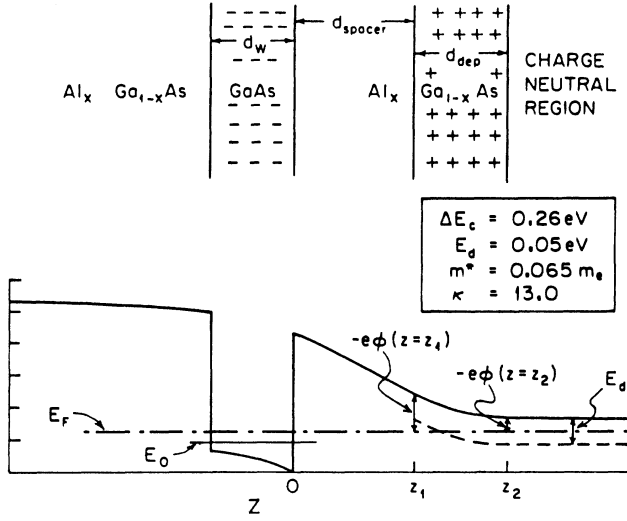


FIG. 1. Schematic of one-side-modulation-doped $\text{Al}_x\text{Ga}_{1-x}\text{As}/\text{GaAs}/\text{Al}_x\text{Ga}_{1-x}\text{As}$ single-quantum-well structure and representation of the associated terms used in the self-consistent calculation of potential distribution.

B. Mobility within memory-function approach

The basic formulation for evaluation of the scattering time (τ) within the memory-function approach has been worked out in detail in Ref. 27. Within this framework the dynamical conductivity is represented as

$$M''(\omega) = \frac{8}{\pi \hbar^2} \left[\frac{1}{N_s} \right] \left[\frac{m^*}{\pi \hbar^2} \right]^2 \left[\frac{Q_I e^2}{\kappa} \right]^2 \int dE_k \int \frac{d\theta}{2\pi} \int dz_i N'_i(z_i) f(E_k) |I_1(E_k, z_i)|^2 \times (\hbar\omega + \{[E_k(E_k - \hbar\omega)]^{1/2} - [E_k(E_k + \hbar\omega)]^{1/2}\} \cos\theta) / \omega, \quad (20)$$

which in the limit $\omega \rightarrow 0$ reduces to

$$M''(\omega \rightarrow 0) = \frac{8}{\pi \hbar} \left[\frac{1}{N_s} \right] \left[\frac{m^*}{\pi \hbar^2} \right]^2 \left[\frac{Q_I e^2}{\kappa} \right]^2 \int dE_k \int \frac{d\theta}{2\pi} \int dz_i N'_i(z_i) f(E_k) |I_1(E_k, z_i)|^2 (1 - \cos\theta). \quad (21)$$

Here,

$$I_1(E_k, z_i) = \frac{\pi}{\lambda_1} \int dz |\eta_0(z)|^2 \frac{e^{-\lambda_1 |z - z_i|}}{\epsilon(E_k)} \quad (22)$$

with

$$\lambda_1 = \left[\frac{8m^* E_k}{\hbar^2} \sin^2(\theta/2) \right]^{1/2}. \quad (23)$$

Here the symbols have the following meaning: z equals the electron coordinate in the confinement direction, z_i the ionized impurity coordinate, θ the scattering angle, E_k the electron energy, $\eta_0(z)$ the electron wave function, $\epsilon(E_k)$ the dielectric response function of quasi-two-dimensionally confined carriers, $f(E_k)$ the Fermi distribution function, $N'_i(z_i)$ the ionized impurity profile, κ

$$\sigma(z) = \left[\frac{i\omega_p^2}{4\pi} \right] [z + M(z)]^{-1}, \quad (15)$$

where $z = \omega + i\delta$ is the complex frequency, ω_p is the plasma frequency, and $M(z) = M' + iM''$ is defined as the memory function. It is given in terms of the current-current correlation function $\langle [j(t), j(0)] \rangle$ via the relations

$$M(z) = z\chi(z)[\chi(z=0) - \chi(z)], \quad (16)$$

$$\chi(z) = -\langle [j, j] \rangle = -i \int_0^\infty e^{izt} \langle [j(t), j(0)] \rangle dt \quad (17)$$

with $\chi(z=0) = N_s/m^*$, where N_s is the electron concentration (per cm^2 in 2D case). The electron scattering time at zero frequency is then given by

$$\tau(\omega=0) = [M''(\omega=0)]^{-1}, \quad (18)$$

so that the low-field dc mobility becomes

$$\mu = (e/m^*) [M''(\omega=0)]^{-1}. \quad (19)$$

The evaluation of $M(z)$ follows straightforwardly the procedure detailed in Ref. 27. Using (33) of Ref. 27, modified for the two-dimensional situation at hand, we obtain the following expression for $M''(\omega)$:

the static dielectric constant of the semiconductor material (which we take to be that of GaAs), Q_I the charge of ionized dopant equal to 1, and m^* the effective mass of electron.

In so far as the dielectric response function $\epsilon(E_k)$ is concerned, we choose a form appropriate for quasi-two-dimensionally confined carriers,³¹

$$\epsilon(E_k) = 1 + [sh(q)/q], \quad (24)$$

where

$$s = 2(m^*/2\pi\hbar^2)(2\pi e^2/\kappa) \quad (25)$$

and

$$q = 2|\mathbf{k}| \sin(\theta/2),$$

\mathbf{k} being the electron wave vector. The function $h(q)$ is

given by

$$h(q) = \int dz_1 \int dz_2 \rho(z_1) \rho(z_2) e^{-q|z_1 - z_2|}, \quad (26)$$

where $\rho(z) = |\eta_0(z)|^2$. Price³¹ has given an interpolation formula for $h(q)$ which does not introduce an error in the transport calculation of more than 10%. This formula is given by³¹

$$h(q) = 1/(1 + bq), \quad (27)$$

where

$$b = \left[2 \int \rho^2(z) dz \right]^{-1}. \quad (28)$$

We employ this formula in our calculations.

III. RESULTS AND DISCUSSION

Figure 2 shows the dependence of the low-temperature electron mobility and carrier concentration in the well on the spacer-layer thickness, for a 100-Å $\text{Al}_{0.33}\text{Ga}_{0.67}\text{As}/\text{GaAs}/\text{Al}_{0.33}\text{Ga}_{0.67}\text{As}$ single-quantum-well structure modulated on one side of the well at a dopant concentration of $5 \times 10^{17} \text{ cm}^{-3}$. This side we take to be the normal-interface side of a grown structure, as also indicated in Fig. 1. It can be seen that increase in the spacer-layer thickness leads to a gradual decrease in the concentration of carriers transferred to the well due to enhancement of the effective barrier for charge transfer. Yet, the mobility increases from $4.77 \times 10^5 \text{ cm}^2/\text{V sec}$ for no spacer case to $2.25 \times 10^6 \text{ cm}^2/\text{V sec}$ for a spacer thickness of 300 Å. This behavior is an interplay of the self-consistent band-bending effects, and the electron wave function and

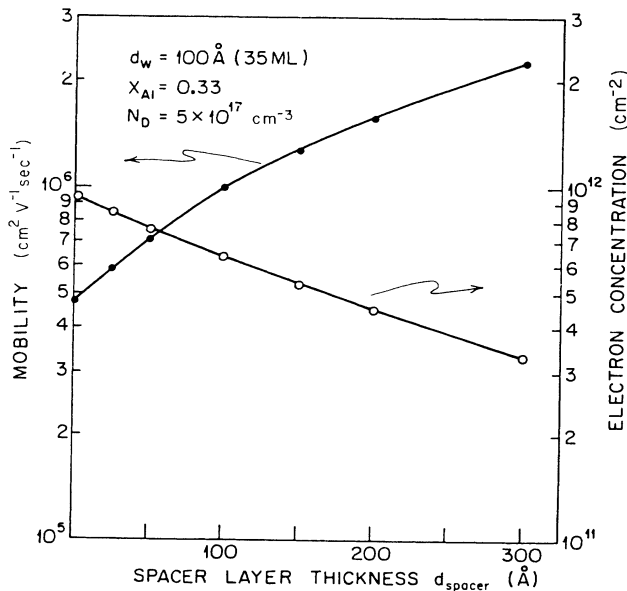


FIG. 2. Dependence of low-temperature electron mobility and carrier concentration in a 100-Å one-side-modulation-doped $\text{Al}_{0.33}\text{Ga}_{0.67}\text{As}/\text{GaAs}/\text{Al}_{0.33}\text{Ga}_{0.67}\text{As}$ quantum-well structure on spacer-layer thickness for a fixed dopant density of $5 \times 10^{17} \text{ cm}^{-3}$.

concentration-dependent mobility parameters such as K_F^{-1} and the screening function $h(q)$, in addition, of course, to the distance dependence of the bare interaction itself. In order to bring out the nature of this interplay we show, in Fig. 3, the potential-energy distributions and wave functions for representative thin (25-Å) and thick (200-Å) spacer-layer situations. Interestingly, the wave functions in the two cases are not significantly different, though $E_F - E_0$ (and thus N_s) is significantly higher for a thinner spacer case. The similarity of the wave functions indicates that the parameter b in the $h(q)$ function defining the screening expression [Eq. (24)] is comparable in the two cases. However, the higher average electron energy attendant to the higher electron concentration for the thin-spacer-layer case leads to a higher degree of screening. Nevertheless, this advantage is negated by the lowering of the average separation between the ionized donors and electrons in this thin spacer case. The net effect is thus a lowering of mobility with decrease in the spacer-layer thickness. An important point to be noted here is the intrinsic coupling of the charge-transfer process with the band-bending effect, which limits the parametric freedom for tailor-making of such configurations. Thus, it is of interest to search for a range of dopant densities for a given range of spacer-layer thicknesses, which could lead to a desired electron concentration in the well.

In Fig. 4 we present the results on the dependence of mobility on spacer-layer thickness for the case wherein the dopant density is changed in such a manner that a

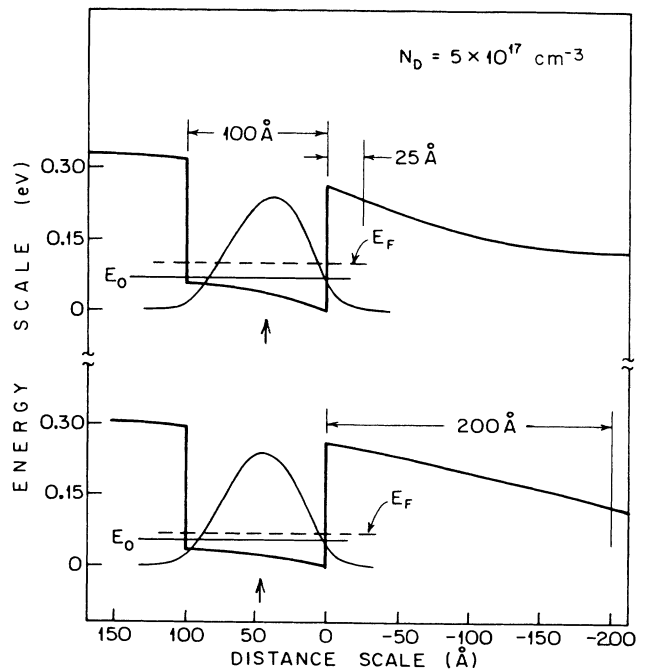


FIG. 3. Potential distributions and electron wave functions for two 100-Å one-side-modulation-doped $\text{Al}_{0.33}\text{Ga}_{0.67}\text{As}/\text{GaAs}/\text{Al}_{0.33}\text{Ga}_{0.67}\text{As}$ quantum-well structures for spacer-layer thicknesses of 25 and 200 Å. The dopant density is $5 \times 10^{17} \text{ cm}^{-3}$. The arrows show the average spatial positions of electron distribution.

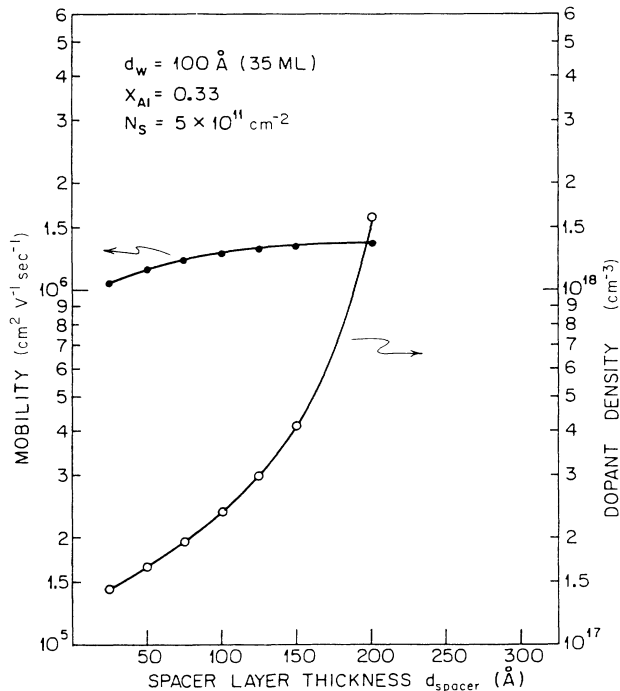


FIG. 4. Dependence of low-temperature electron mobility and the dopant density required to maintain a fixed electron concentration ($5 \times 10^{11} \text{ cm}^{-2}$) in a one-side-modulation-doped $\text{Al}_{0.33}\text{Ga}_{0.67}\text{As}/\text{GaAs}/\text{Al}_{0.33}\text{Ga}_{0.67}\text{As}$ quantum well, on the spacer-layer thickness.

fixed electron concentration of $5 \times 10^{11} \text{ cm}^{-2}$ is attained in the quantum well. These results are, once again, for a 100- \AA $\text{Al}_{0.33}\text{Ga}_{0.67}\text{As}/\text{GaAs}/\text{Al}_{0.33}\text{Ga}_{0.67}\text{As}$ quantum-well modulation doped only on the normal-interface side. It can be readily seen that as the spacer-layer thickness is increased it becomes increasingly difficult to achieve a given electron concentration in the well¹⁸ due to an attendant increase in the effective strength of the barrier for charge transfer. Thus almost an order of magnitude (from 10^{17} to 10^{18} cm^{-3}) increase in dopant density is required to maintain a fixed electron concentration of $5 \times 10^{11} \text{ cm}^{-2}$ in the well as the spacer thickness is increased from ~ 25 to $\sim 200 \text{ \AA}$. Of course, the magnitude of the range of dopant density required to maintain a fixed electron concentration in the well is a function of the desired electron concentration itself and the width of the well. In so far as the variation of mobility with increase in spacer thickness is concerned, one has an interplay of the positive contribution from the increase in the effective separation between the scatterers and the carriers, and a negative contribution from the increase in the density of dopant needed to keep the carrier constant in the well. Clearly, the latter starts becoming increasingly important for spacer thicknesses of greater than $\sim 100 \text{ \AA}$.

Next, we address the interesting question of quantum-size effects in such a one-sided doped structure. In our previous theoretical studies on symmetrically (uniformly and modulation) doped,^{29,36} single quantum wells carried

out without incorporating band-bending effects and the electron-electron interaction, we had demonstrated that the well-width dependence of the electron wave function and the attendant modification of the screening effects have a major influence on the nature and degree of quantum-size effects. In the present case of a one-sided-doped well the band-bending effects are crucial to the charge-transfer process itself and since the electric field in the spacer region depends on the density distribution of electrons in the well, the band bending is influenced by the size of the quantum well and thus contributes an interesting feature to the aspect of quantum-size effects. Clearly these effects are bound to be more important (not necessarily dominant) in single-side-doped quantum wells as compared to the case of symmetrically doped wells.

In Fig. 5 we show the dependence of the low-temperature electron mobility and the electron concentration on the width of the quantum well for a fixed spacer-layer thickness of 150 \AA (solid lines) and a fixed dopant density of $5 \times 10^{17} \text{ cm}^{-3}$. The barrier-layer Al concentration in these structures is 33%. Before we discuss the size effect in this case it is important to mention that the size effect does depend on such parameters as the dopant density, spacer-layer thickness, and the Al concentration in the barrier layer. In the representative case shown here it may be seen that a decrease in the width of the quantum well leads to a significant and in-

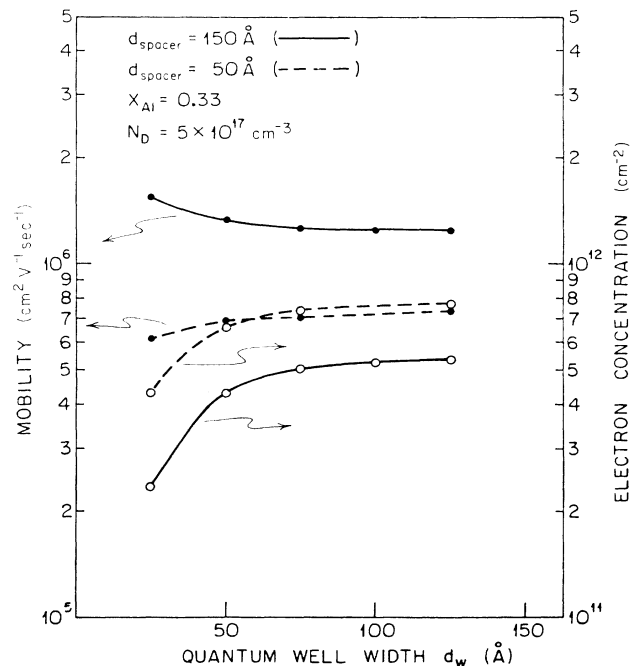


FIG. 5. Variation of the low-temperature electron mobility and electron concentration in the well as a function of the width of the one-side-modulation-doped $\text{Al}_{0.33}\text{Ga}_{0.67}\text{As}/\text{GaAs}/\text{Al}_{0.33}\text{Ga}_{0.67}\text{As}$ quantum-well structure for two cases of spacer-layer thickness, viz. $d_{\text{spacer}} = 50 \text{ \AA}$ and $d_{\text{spacer}} = 150 \text{ \AA}$. The dopant density is fixed at $5 \times 10^{17} \text{ cm}^{-3}$.

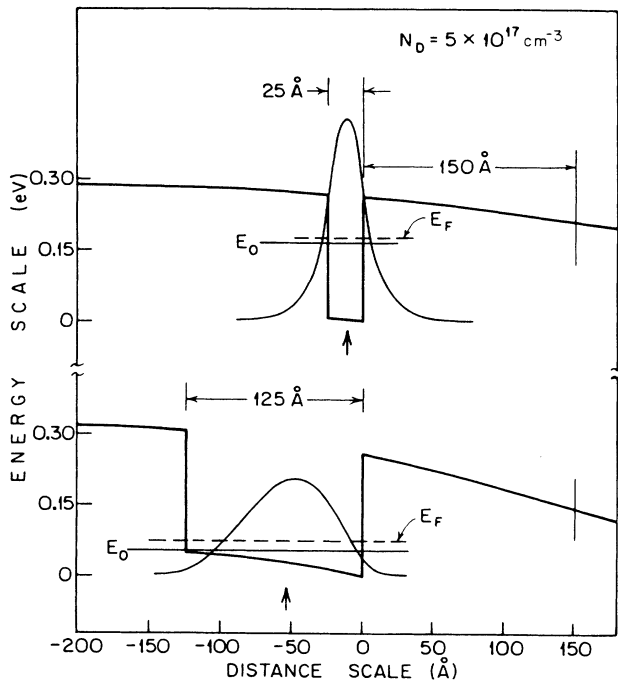


FIG. 6. Potential distributions and electron wave functions for two one-side-modulation-doped $\text{Al}_{0.33}\text{Ga}_{0.67}\text{As}/\text{GaAs}/\text{Al}_{0.33}\text{Ga}_{0.67}\text{As}$ single-quantum-well structures having well widths of 25 and 125 Å. The spacer-layer thickness is 150 Å for both the cases and the dopant density is fixed at $5 \times 10^{17} \text{ cm}^{-3}$. The arrows show the average spatial positions of electron distribution.

creasingly faster decrease in the electron concentration in the quantum well below a well width of ~ 75 Å. This is also associated with a gradual increase in the value of low-temperature mobility. In order to understand the mechanisms contributing to this rather interesting size effect, we plot in Fig. 6 the potential distribution and electron wave functions for wells having widths of 25 and 125 Å, which typically corresponds to thin and thick wells, respectively, in the quantum-size-effect regime. It can be clearly seen that the average separation between the electron distribution and the ionized donors is larger in the case of the 125-Å well than the 25-Å well and also $E_F - E_0$ is higher in the former case as compared to the latter. Both these effects have an effect on the mobility which tends to enhance its value more for the 125-Å-well case than for the 25-Å-well case. However, the calculated mobility is higher for $d_w = 25$ Å, which indicates that the screening effect characteristic of quasi-two-dimensional confinement of electrons, especially the role of the parameter $h(q)$, is important in

influencing the size effect. The calculated values of the parameter b in Eq. (28) evaluated for 25- and 125-Å wells are 28.8 and 51.85 Å, respectively, and it clearly leads to a stronger screening in the case of 25-Å well. This effect overshadows the other two effects mentioned above and the mobility gradually rises as the width of the well is decreased. It can be expected that for a smaller value of spacer-layer thickness the effect of decrease in the separation between the ionized dopants and the average electron location with decrease in the well width should dominate over the modification rendered to the screening. That this indeed is the case can be seen from the size effect for a 50-Å spacer case shown by dotted lines in Fig. 5.

IV. CONCLUSION

In conclusion, we have presented theoretical results for the low-temperature electron mobility limited by remote ionized impurity scattering in one-side-doped $\text{Al}_{0.33}\text{Ga}_{0.67}\text{As}/\text{GaAs}/\text{Al}_{0.33}\text{Ga}_{0.67}\text{As}$ single-quantum-well structures. The results are obtained employing a self-consistent band-bending and quantum-state calculation within the memory-function approach. The dependence of mobility on the spacer thickness, the dopant density, and the width of the well is investigated, and their corresponding consequences for situations of experimental interest are brought out. The influence of other scattering mechanisms, such as alloy disorder^{18,28} and interface roughness,^{18,36,37} on the mobilities calculated here needs to be examined. Previous theoretical studies of electron transport in symmetrically modulation-doped quantum wells and superlattices show that remote ion scattering is the dominant scattering mechanism in such structures when the quantum confinement length scales are over 80 to 100 Å. For thinner confinement lengths alloy disorder and interface roughness can have significant contributions to low-temperature electron mobility. We have undertaken a comprehensive study of the origin and growth condition dependence of such disorders via Monte Carlo simulations of molecular-beam-epitaxy growth and implications of the quantitative information derived therefrom on the confined carrier properties such as luminescence,³⁸ transport, etc. The results of such studies on the low-temperature electron mobility in one-side-modulation-doped structures will be reported in a subsequent publication.

ACKNOWLEDGMENT

This work was supported by the U.S. Army Research Office.

*Permanent address: Department of Physics, Poona University, Pune, India.

¹See, for example, A. C. Gossard, in *Thin Films: Preparation and Techniques*, edited by K. N. Tu and R. Rosenberg

(Academic, New York, 1982), Vol. 24.

²See, for example, Proceedings of the First International Conference on Metastable and Modulated Semiconductor Structures, edited by F. J. Grunthner and A. Madhukar [J.

- Vac. Sci. Technol. B **1**, 217 (1983)].
- ³F. Capasso, *Ann. Rev. Mater. Sci.* **16**, 261 (1986), and references therein.
- ⁴F. Capasso, K. Mohammed, and A. Y. Cho, *IEEE J. Quant. Electron.* **QE-22**, 1853 (1986).
- ⁵R. Dingle, H. L. Stormer, A. C. Gossard, and W. Wiegmann, *Appl. Phys. Lett.* **33**, 665 (1978).
- ⁶L. C. Witkowski, T. J. Drummond, C. M. Stanchak, and H. Morkoc, *Appl. Phys. Lett.* **37**, 1033 (1980).
- ⁷H. L. Stormer, A. Pinczuk, A. C. Gossard, and W. Wiegmann, *Appl. Phys. Lett.* **38**, 691 (1981).
- ⁸S. Hiyamizu, J. Saito, K. Kondo, T. Yamamoto, T. Ishikawa, and S. Sasa, *J. Vac. Sci. Technol. B* **3**, 585 (1985).
- ⁹G. Weimann and W. Schlapp, *Appl. Phys. Lett.* **46**, 411 (1985).
- ¹⁰M. Heiblum, E. E. Mendez, and F. Stern, *Appl. Phys. Lett.* **44**, 1064 (1984).
- ¹¹E. E. Mendez, P. J. Price, and M. Heiblum, *Appl. Phys. Lett.* **45**, 294 (1984).
- ¹²E. F. Schubert, K. Ploog, H. Dambkes, and K. Heime, *Appl. Phys. A* **33**, 63 (1984).
- ¹³S. Hiyamizu and T. Mimura, *J. Cryst. Growth* **56**, 455 (1982).
- ¹⁴T. J. Drummond, H. Morkoc, S. L. Su, R. Fischer, and A. Y. Cho, *Electron. Lett.* **17**, 870 (1981).
- ¹⁵T. J. Drummond, J. Klem, D. Arnold, R. Fisher, R. E. Thorne, W. G. Lyons, and H. Morkoc, *Appl. Phys. Lett.* **42**, 615 (1983).
- ¹⁶H. Morkoc, T. J. Drummond, R. E. Thorne, and W. Kopp, *Jpn. J. Appl. Phys.* **20**, L913 (1981).
- ¹⁷M. Heiblum, *J. Vac. Sci. Technol. B* **3**, 820 (1985).
- ¹⁸T. Ando, *J. Phys. Soc. Jpn.* **51**, 3900 (1982).
- ¹⁹S. Sasa, J. Saito, K. Nanbu, T. Ishikawa, and S. Hiyamizu, *Jpn. J. Appl. Phys.* **23**, L573 (1984).
- ²⁰S. Sasa, J. Saito, K. Nanbu, T. Ishikawa, S. Hiyamizu, and M. Inoue, *Jpn. J. Appl. Phys.* **24**, L281 (1985).
- ²¹K. Inoue, H. Sakaki, J. Yoshino, and Y. Yoshioka, *Appl. Phys. Lett.* **46**, 973 (1985).
- ²²A. Rockett, J. Klem, S. A. Barnett, J. E. Greene, and H. Morkoc, *J. Appl. Phys.* **59**, 2777 (1986).
- ²³H. Burkhard, W. Schlapp, and G. Weimann, *Surf. Sci.* **174**, 387 (1986).
- ²⁴M. H. Meynadier, J. Orgonasi, C. Delalande, J. A. Brum, G. Bastard, M. Voos, G. Weimann, and W. Scalapp, *Phys. Rev. B* **34**, 2482 (1986).
- ²⁵L. Hedin and B. I. Lundquist, *J. Phys. C* **4**, 2064 (1971).
- ²⁶F. Stern and S. D. Sarma, *Phys. Rev. B* **30**, 840 (1984).
- ²⁷W. Gotze and P. Wolfe, *Phys. Rev. B* **6**, 1226 (1972).
- ²⁸S. B. Ogale and A. Madhukar, *J. Appl. Phys.* **56**, 368 (1984).
- ²⁹S. B. Ogale and A. Madhukar, *J. Appl. Phys.* **55**, 483 (1984).
- ³⁰A. Gold, *Phys. Rev. B* **35**, 723 (1987).
- ³¹P. J. Price, *J. Vac. Sci. Technol.* **19**, 599 (1981).
- ³²T. Ando, *J. Phys. Soc. Jpn.* **51**, 3893 (1982).
- ³³K. Inoue, H. Sakaki, J. Yoshino, and T. Hotta, *J. Appl. Phys.* **58**, 4277 (1985).
- ³⁴K. Lee, M. Shur, T. J. Drummond, and H. Morkoc, *J. Appl. Phys.* **54**, 2093 (1983).
- ³⁵K. Miyatsuji, H. Hihara, and C. Hamaguchi, *Superlatt. Microstruc.* **1**, 43 (1985).
- ³⁶S. B. Ogale and A. Madhukar (unpublished).
- ³⁷S. Mori and T. Ando, *J. Phys. Soc. Jpn.* **48**, 865 (1977).
- ³⁸S. B. Ogale, F. Voillot, M. Thomson, T. C. Lee, W. C. Tang, P. Chen, and J. Y. Kim, *Phys. Rev. B* **36**, 1662 (1987).